Journal of Orthopaedic Translation 51 (2025) 163–175

Contents lists available at ScienceDirect

Journal of Orthopaedic Translation

journal homepage: www.journals.elsevier.com/journal-of-orthopaedic-translation

Original article

Inhibition of ERK1/2 mediated activation of Drp1 alleviates intervertebral disc degeneration via suppressing pyroptosis and apoptosis in nucleus pulposus cells

Shenkai Su [a,b,c,1], Xuanzhang Wu [a,b,c,1], Bin Li [d,1], Fengyu Zhang [b], Kaiying Zhang [b], Hui Wang [c,e,***], Yan Lin [a,b,c,**], Jiaoxiang Chen [a,b,c,*]

[a] Department of Orthopaedics, The Second Affiliated Hospital and Yuying Children's Hospital of Wenzhou Medical University, Wenzhou, Zhejiang Province, China
[b] The Second School of Medicine, Wenzhou Medical University, Wenzhou, Zhejiang Province, China
[c] Zhejiang Provincial Key Laboratory of Orthopaedics, Wenzhou, Zhejiang Province, China
[d] Department of Orthopaedics, Yuhuan People's Hospital, Taizhou, Zhejiang Province, China
[e] Institute of Autoimmune Diseases, School of Basic Medical Sciences, Wenzhou Medical University, Wenzhou, Zhejiang, China

ARTICLE INFO

Keywords:
Drp1
Mitochondria
Apoptosis
Pyroptosis
IVDD

ABSTRACT

Objective: Dynamin-related protein 1 (Drp1) plays a crucial role in various inflammatory and degenerative diseases, yet its involvement in intervertebral disc degeneration (IVDD) remains poorly understood. This study aims to elucidate the mechanism by which Drp1 contributes to IVDD and to identify the efficacy of the Drp1 inhibitor Mdivi-1 on IVDD.

Methods: Tert-butyl hydroperoxide (TBHP) is utilized to induce an oxidative stress microenvironment *in vitro*. *In vivo*, IVDD model is constructed in 8-week old rats through puncture operation. The therapeutic effect of Mdivi-1 is evaluated through X-ray, MRI and histological analysis. A comprehensive set of experiments, including single-cell sequencing analysis, western blot, flow cytometry and immunofluorescence staining, are conducted to investigate the role and underlying mechanisms of Drp1 *in vitro*.

Results: Our study demonstrates that the expression of Drp1 and phosphorylated Drp1 (p-Drp1) are up-regulated in degenerative nucleus pulposus cells (NPCs), which are accompanied with increased pyroptosis and apoptosis. *In vivo*, both si-Drp1-mediated Drp1 knockdown and the pharmacological inhibitor Mdivi-1 alleviate puncture-induced IVDD in rats. *In vitro*, si-Drp1 or Mdivi-1 inhibits mitochondria-dependent apoptosis and pyroptosis triggered by TBHP. Mechanistically, Mdivi-1 reduces p-Drp1 levels, inhibits excessive mitochondrial fission, and mitigates mitochondrial dysfunction. Drp1 phosphorylation-based Drp1 mitochondrial translocation and subsequent apoptosis and pyroptosis are regulated by ERK1/2 phosphorylation in NPCs under oxidative stress condition.

Conclusion: This study highlights the involvement of Drp1 in the pathological progression of degenerative NPCs in IVDD, which is regulated by ERK1/2. Pharmacological inhibition of Drp1 with Mdivi-1 protects NPCs by promoting mitochondrial function and attenuating apoptosis and pyroptosis. These findings suggest that Mdivi-1 is a promising therapeutic candidate for IVDD treatment.

Translational Potential: By offering experimental evidence on the role and mechanism of Drp1 in IVDD, this study underscores the potential of Mdivi-1 as a therapeutic strategy for IVDD.

* Corresponding author. Department of Orthopaedics, The Second Affiliated Hospital and Yuying Children's Hospital of Wenzhou Medical University, Wenzhou, Zhejiang Province, China.
** Corresponding author. Department of Orthopaedics, The Second Affiliated Hospital and Yuying Children's Hospital of Wenzhou Medical University, Wenzhou, Zhejiang Province, China.
*** Corresponding author. Zhejiang Provincial Key Laboratory of Orthopaedics, Wenzhou, Zhejiang Province, China.
E-mail addresses: wh060550@163.com (H. Wang), wzlinyan@126.com (Y. Lin), jiaoxiangchen@wmu.edu.cn (J. Chen).
[1] Shenkai Su, Xuanzhang Wu and Bin Li are co-first authors who equally contributed to this manuscript.

https://doi.org/10.1016/j.jot.2025.01.013
Received 17 September 2024; Received in revised form 15 December 2024; Accepted 12 January 2025

1. Introduction

Lower back pain represents a major global health challenge, leading to considerable social and economic burdens [1]. By 2050, it is estimated that over 800 million people worldwide will suffer from lower back pain, with intervertebral disc degeneration (IVDD) being a key factor in its onset [2]. IVDD is a multifactorial condition influenced by a variety of factors such as obesity, malnutrition, and abnormal stress, yet its precise pathogenesis remains unclear, and effective treatments are currently unavailable [3]. The intervertebral disc is composed of the endplate, nucleus pulposus (NP), and annulus fibrosus. The reduction of nucleus pulposus cells (NPCs), as resident cells of NP tissues, is an important pathological feature of IVDD. Understanding the molecular mechanisms underlying NPC cell death may offer valuable insights into the treatment of IVDD.

Mitochondrial dysfunction is involved in various pathophysiological processes in multiple diseases, including ATP synthesis, reactive oxygen species (ROS) metabolism, calcium homeostasis, intrinsic apoptosis and pyroptosis [4]. Pathogenic factors such as oxidative stress induce mitochondrial dysfunction by impairing the mitochondrial capacity to eliminate ROS, thereby establishing a vicious cycle of increased intracellular oxidative stress [5,6]. Elevated mitochondrial ROS level results in a decrease in MMP (MMP), the opening of the mitochondrial permeability transition pore (mPTP) and the increase of mitochondrial membrane permeability. Consequently, cytochrome c is released from the mitochondria into the cytoplasm, thereby activating pro-apoptotic factors such as caspase-9 and caspase-3, triggering intrinsic apoptosis [7]. Furthermore, increased mitochondrial membrane permeability facilitates the release of mitochondrial DNA (mtDNA) into the cytoplasm, where it acts as a pathogen- or damage-associated molecular pattern (PAMP or DAMP), detected by pattern recognition receptors. This activation triggers a type I immune response [8]. A previous study highlighted that cGAS served as a primary receptor for double-stranded DNA (dsDNA) in the cytoplasm of NPCs. The activation of the cGAS-Sting axis promoted apoptosis, cellular senescence, and extracellular matrix degradation in NPCs [9,10]. Additionally, the mPTP opening contributed to the release of mtDNA into the cytoplasm, following the activation of the cGAS-Sting axis and triggering NLRP3-related pyroptosis in NPCs under oxidative stress, along with the exacerbation of IVDD progression [11]. However, the precise mechanisms underlying the mPTP opening and the increase of mitochondrial permeability remain poorly understood.

Mitochondrial dynamics (including mitochondrial fusion and fission) are crucial for maintaining mitochondrial quality. These processes are regulated by mitochondrial fusion-related proteins (MFN1, MFN2, OPA1) and fission-related proteins (Drp1, Fis1, Mff, MiD49 and MiD51) [12]. In mitochondrial fission, the key driver of mitochondrial fission is dynamin-related protein 1 (Drp1), which is a GTP enzyme predominantly located in the cytoplasm, but translocates to the outer mitochondrial membrane upon activation, where it facilitates mitochondrial division [13]. The involvement of Drp1 in excessive mitochondrial fission has been identified in multiple diseases, leading to mitochondrial fragmentation and cellular dysfunction, which are characterized by elevated ROS levels and disrupted energy metabolism [14]. Increasing evidence has shown that excessive mitochondrial fission in NPCs contributes to IVDD pathology. However, the underlying mechanism, particularly concerning oxidative stress-induced apoptosis and pyroptosis in NPCs, remains unclear [15].

The objective of this study is to investigate the role of Drp1 in NPCs in the context of IVDD. Specifically, we seek to analyze human nucleus pulposus (HNP) tissue samples to explore the expression and correlation between Drp1 and pyroptosis or apoptosis. Additionally, we intend to examine the role of oxidative stress in Drp1 activation, as well the role of Drp1 in the modulation of apoptosis and pyroptosis in NPCs through both HNP tissue sample analysis and cellular experiments. Finally, we will assess the therapeutic potential of Drp1 deficiency in a rat puncture-induced IVDD model.

2. Material and methods

2.1. Ethics statement

In this study, HNP tissue collection was approved by the Medical Ethics Committee of the Second Affiliated Hospital and Yuying Children's Hospital of Wenzhou Medical University (Approval No. LCKY2020-20). Informed consent was obtained from all patients according to the *Declaration of Helsinki*. The animal experiments were approved by the Laboratory Animal Ethics Committee of Wenzhou Medical University (Approval No. wydw2020-0165).

3. Antibodies and reagents

A list of the antibodies and reagents used in this study is provided in Supplemental Table 1.

3.1. Single-cell RNA sequence (scRNA-seq) analysis

The scRNA-seq dataset (GSE153066), including eight control and eight degenerative nucleus pulposus samples, was retrieved from the GEO database (https://www.ncbi.nlm.nih.gov/geo). The dataset was processed with the standard 10x Genomics protocol as previously described [16]. Low-quality cells were excluded from analysis if they exhibited fewer than 200 or more than 6000 detected genes, as abnormal gene counts in barcodes suggest the presence of dying cells, cells with compromised membranes, or cell doublets. Additionally, cells with a mitochondrial gene mapping rate of more than 15 % were also excluded, as this may indicate a high degree of cell membrane compromise and mRNA leakage.

The remaining high-quality cells were normalized and scaled using the "NormalizeData" and "ScaleData" functions, with a view to achieve linear conversion. Principal component analysis (PCA) was carried out on the top 2000 variable genes, and the 20 most statistically significant principal components were selected for subsequent clustering. Batch effects were mitigated by integrating the scRNA-seq data from multiple samples using the "RunHarmony" function from the Harmony package. The resulting clusters were then visualized using Uniform Manifold Approximation and Projection (UMAP). In order to identify these clusters, a weighted Shared Nearest Neighbor (SNN) graph-based method was adopted. Marker genes for each cluster were identified using the Wilcoxon rank-sum test (with the default parameters: "bimod", likelihood-ratio test, $p \leq 0.01$) via the "FindAllMarkers" function in Seurat. These markers were selected based on expression in at least 10 % of the cells within a cluster and an average log2 fold change (FC) greater than 0.25. Differentially expressed genes (DEGs) were determined with a $|\log2\ FC| > 0.25$ and parametric F-tests comparing nested linear models (p value < 0.05), via the "FindMarkersc" function. A GO functional enrichment analysis was performed using the "clusterProfiler" package, applying a significance threshold of $p < 0.05$ and a gene count ≥ 2.

3.2. Human nucleus pulposus (HNP) samples collection

A total of 24 HNP samples (6 per group) were collected from patients undergoing spinal surgery. The degree of IVDD was assessed using the Pfirrmann grading system. Grade I and Grade II HNP samples were collected from patients with thoracolumbar vertebral fractures, while Grade IV and Grade V samples were obtained from patients with degenerative disc disease. Detailed information on the samples is provided in Supplemental Table 2.

3.3. Rat puncture-induced IVDD model and grouping

8-week-old male Sprague–Dawley (SD) rats were utilized in the present study. Anesthesia was administered via injection of 2 % (w/v) pentobarbital (40 mg/kg). A puncture-induced IVDD model was established as previously described [10,11]. Briefly, after localization of the tail disc (Co7/8) via X-ray radiography, utilizing a 21G needle, the annulus fibrosus was punctured perpendicularly (5 mm) with a 360° rotation maintained for 1 min. The rats were then randomly divided into four groups: control, IVDD, IVDD + si-Drp1, and IVDD + Mdivi-1. In the IVDD + si-Drp1 group, 3 μL of si-Drp1 was injected into the center of the nucleus pulposus, while the rats in the IVDD + Mdivi-1 group received an intraperitoneal injection of Mdivi-1 (3 mg/kg, MedChemExpress) dissolved in DMSO. 8 weeks after surgery, X-ray and MRI imaging were performed, and the disc samples were collected for further histological experiments.

3.4. X-ray and MRI imaging

8 weeks after surgery, X-ray and MRI images were obtained. X-ray imaging was performed through an X-ray irradiation system (Kubtec, USA), and the disc height index (DHI) was calculated as described in our previous study [17]. T2-weighted MRI sequences were acquired using a 3.0 T magnet (Philips Intera Achieva 3.0 MR, Netherlands) to evaluate the Pfirrmann grade by assessing the signal intensity of the nucleus pulposus and structural changes in the intervertebral discs.

3.5. Histological analysis

The rats were sacrificed, and the Co7/8 punctured discs were harvested at 8 weeks after surgery. The disc samples were fixed in 4 % paraformaldehyde for 24 h, followed by decalcification in EDTA decalcifying solution for 4 weeks. The discs were then dehydrated and embedded in paraffin for sectioning. The sections were stained using Hematoxylin-Eosin (HE) and Safranin O-Fast Green (SO) to assess the morphology of the nucleus pulposus, annulus fibrosus and endplate. The images of the HE and SO stained sections were captured using a light microscope (Olympus Inc., Japan), and the histological score was determined in a blinded manner based on previously established criteria.

3.6. Immunofluorescence and immunohistochemical analysis of nucleus pulposus tissues

The human and rat NP tissue sections were deparaffinized and rehydrated for subsequent immunofluorescence and immunohistochemistry (IHC). For IHC, H_2O_2 and pepsin incubation were performed before goat serum blocking. After a 1 h blocking with goat serum at 37 °C, the sections were incubated overnight at 4 °C with primary antibodies. Following PBS washes, the sections were incubated with either Alexa Fluor-conjugated secondary antibodies and DAPI, or HRP-conjugated secondary antibodies and DAB.

3.7. Measurement of ROS levels in human nucleus pulposus tissues

The ROS level in human HNP tissues was measured using the DCFH-DA assay kit. The sections were then stained as per the manufacturer's instructions. The images were acquired by fluorescence microscopy (Olympus Inc., Tokyo, Japan) and analyzed using Image J 2.1 (Bethesda, USA).

3.8. Isolation and culture of rat NPCs

Forty male SD rats (6 weeks old) were selected for NPCs isolation and culture. After euthanasia using 10 % chloral hydrate, the NP tissues were carefully dissected and collected under sterile conditions. After that, the tissues were digested with 0.1 % type II collagenase at 37 °C for 4 h. The NPCs were collected after centrifugation, cultured in DMEM/F12 medium supplemented with 15 % FBS and 1 % penicillin/streptomycin antibiotics in an incubator (37 °C, 5 % CO_2). NPCs at passages 1–3 were used for subsequent cellular experiments.

3.9. Western blot analysis

The HNP tissues and conditionally treated NPCs were harvested and lysed using RIPA buffer (Beyotime) for protein extraction. The protein samples (30–60 μg) were separated by 7.5 %–12.5 % SDS-PAGE and transferred to PVDF membranes. After blocking with 5 % non-fat milk for 2 h at room temperature, the membranes were incubated with primary antibodies overnight at 4 °C. The membranes were then washed with PBS and incubated with secondary antibodies for 2 h at 37 °C. The protein bands were visualized and quantified using the Chemi DocXRS Imaging System and ImageJ 2.1 software.

3.10. Measurement of mitochondrial ROS and MMP

Mitochondrial ROS and MMP were measured using MitoSOX and JC-1 assay kits. Briefly, according to the manufacturer's protocols, NPCs were stained after conditional treatment, and images were captured using a fluorescence microscope for analysis.

3.11. Flow cytometry assay

The apoptosis ratio of NPCs was determined with an Annexin V/PI assay kit, following the manufacturer's instructions. To assess the pyroptosis ratio in NPCs, pre-treated NPCs were stained with 7-AAD and anti-caspase-1 antibodies. Flow cytometry was performed using a Beckman Coulter CytoFlex flow cytometer (Beckman, IN, USA) and the data were analyzed using FlowJo software.

3.12. Immunohistochemical and immunofluorescent analysis of NPCs

The cultured NPCs were then treated according to the study proposal. Following treatment, the NPCs were fixed, permeabilized, blocked and incubated with primary antibodies overnight at 4 °C. For IHC, the NPCs were treated with H_2O_2, pepsin, goat serum, HRP-conjugated secondary antibody and DAB staining, followed by dehydration, similar to the protocol used for HNP tissues. For immunofluorescent staining, the NPCs were incubated using Alexa Fluor-conjugated secondary antibodies, MitoTracker Red and DAPI, mirroring the procedures for the HNP tissues. The images were captured with a fluorescence microscope (Olympus Inc., Tokyo, Japan). Quantification of mtDNA release was conducted as previously reported [18].

3.13. Small-interfering RNA (si-RNA) transfection

si-RNA targeting the Drp1 gene (si-Drp1) was purchased from RiboBio (Guangzhou, China). The si-Drp1 sequence was showed in Supplementary Table 3. The si-Drp1 transfection was conducted as previously described [19,20]. *In vitro*, the pre-treated NPCs seeded in 12-well plates were transfected with si-Drp1 using Lipofectamine™ 2000 transfection reagent, following the manufacturer's instructions. *In vivo*, 2 μL of si-Drp1 was injected intradiscally into the nucleus pulposus tissues of rats through a microliter syringe with a 27G needle.

3.14. Statistical analysis

The data are expressed as the Mean ± SD. Statistical analyses were conducted using SPSS software version 18.0. The normality of continuous variables was evaluated. For normally distributed data with equal variances, one-way analysis of variance (ANOVA) followed by Tukey's post-hoc test was performed for comparison between control and

treatment groups. Student's t-test was adopted for comparison between two groups. For non-parametric data, the Kruskal–Wallis H test was applied. Simple linear regression was performed to evaluate the relationship between two variables. $P < 0.05$ was considered statistically significant.

4. Results

4.1. Increased Drp1 expression and activation of pyroptosis and apoptosis in IVDD

Given that the NP tissues played a primary role in intervertebral disc and that NPCs were resident cells of NP tissues, we carried out scRNA-seq analysis and biological experiments to identify the mRNA level of Drp1 and investigate the pathological changes in degenerative NP tissues. The volcano plot demonstrated that the gene expression of Drp1 was up-regulated in degenerative NP tissues (Fig. 1A). Previous studies have confirmed various immune cell infiltrations and fibrous tissue hyperplasia in NP tissues. We further carried out scRNA-seq to determine whether Drp1 was similarly up-regulated in degenerative NPCs. The UMAP clustering analysis indicated that the mRNA expression of Drp1 was predominantly localized in NP tissues area (Fig. 1B and C). The NP clusters were then classified into four distinct groups: COL2A1 NPCs, COL6A3 NPCs, ORM1 NPCs, and FTH1 NPCs (Fig. 1D). The mRNA expression of Drp1 was up-regulated in COL2A1 NPCs, COL6A3 NPCs and FTH1 NPCs (Fig. 1E and F). Furthermore, we collected HNP tissues from low degenerative (Pfirrmann Grade I) and high degenerative (Pfirrmann Grade IV) discs and performed histological staining to identify whether the protein expression of Drp1 was increased in degenerative NPCs. Histological staining suggested that degenerative NP tissues (Grade IV) manifested cellular aggregation, cartilage cyst-like structures, and a marked disruption of nuclear matrix architecture (Fig. 1G). Immunofluorescence results further confirmed that the protein expression of Drp1 was increased in degenerative NPCs, as well as mRNA (Fig. 1H). We then established rats punctured-induced IVDD model (8 weeks), and the immunofluorescence result revealed an increased expression of Drp1 in NPCs in IVDD model, consistent with the finding in the HNP tissues (Fig. 1I and J). These data implied that Drp1 played a role in IVDD. To explore the underlying etiological factors contributing to NPC dysfunction in IVDD, we performed a GO analysis, which revealed a substantial enrichment of apoptosis and pyroptosis signaling pathways in degenerative NPCs (Fig. 1K). We then carried out western blot analysis to determine the protein levels of Drp1, apoptosis-associated molecules (cleaved caspase-3), and pyroptosis-associated molecules (NLRP3 and cleaved caspase-1) across different degenerative HNP tissues. The western blot results indicated notably increased expressions of Drp1, cleaved caspase-1, NLRP3, and cleaved caspase-3 in degenerative HNP tissues (Fig. 1L and M). Linear regression analysis further demonstrated that higher protein expressions of Drp1, cleaved caspase-1, NLRP3, and cleaved caspase-3 were correlated with more severe IVDD (Fig. 1N). Since Drp1 played a key role in cellular homeostasis, we also further explored the relation between Drp1 and apoptosis or pyroptosis. The linear analysis unveiled a positive correlation between Drp1 and cleaved caspase-1, NLRP3, or cleaved caspase-3 (Fig. S1). These findings underscored that IVDD was accompanied by increased Drp1 expression and escalating pyroptosis and apoptosis processes.

4.2. Accumulated oxidative stress increases Drp1 expression and triggers pyroptosis and apoptosis in NPCs

In the pathogenesis of IVDD, various pathological factors contribute to elevated oxidative stress level, which plays a key role in the survival of NPCs. Previous studies have documented the activation of pyroptosis and apoptosis in degenerative HNP tissues [10,16,21]. In this study, we sought to investigate whether elevated oxidative stress level was associated with the occurrence of pyroptosis and apoptosis in NPCs, using HNP tissues and cellular experiments. In HNP samples, IHC was carried out to determine the expressions of Drp1, cleaved caspase-1, NLRP3, and cleaved caspase-3. Additionally, the ROS level in HNP tissues was measured using a DCFH-DA probe (Fig. 2A). Linear regression analysis revealed a significant positive connection between oxidative stress and Drp1, cleaved caspase-1, NLRP3 or cleaved caspase-3 (Fig. 2B). *In vitro*, NPCs were cultured and treated with different concentrations of TBHP (0, 20, and 40 μM), with a view to investigate the cellular response under oxidative stress through western blot and flow cytometry assay. Western blot analysis suggested a dose-dependent increase in Drp1 expression, along with apoptosis-related markers (cleaved caspase-3 and cytochrome c) and pyroptosis-related markers (NLRP3, ASC NT-GSDMD and cleaved caspase-1) following TBHP treatment (Fig. 2C and D). The flow cytometry analysis of Annexin V/PI revealed a significant increase in the apoptosis ratio of NPCs, particularly in the late stage of apoptosis, following TBHP treatment (Fig. 2E and F). 7-AAD is a nucleic acid dye binding to DNA, and its binding increases, with the gradual increase of the permeability of the plasma membrane to 7-AAD during cell death. The NPCs were labeled with 7-AAD and anti-caspase-1, and cells positive for both 7-AAD and caspase-1 were identified as undergoing pyroptosis. A dose-dependent increase in the ratio of 7-AAD^{+}/cleaved caspase-1^{+} cells was noted in TBHP-treated NPCs (Fig. 2G and H). These data collectively suggested that accumulated oxidative stress up-regulated Drp1 expression, leading to the activation of apoptosis and pyroptosis in NPCs.

4.3. Drp1 deficiency ameliorates IVDD progression in rats puncture-induced IVDD model

Having established the association between oxidative stress and apoptosis or pyroptosis with up-regulation of Drp1 in NPCs (Fig. 2), we then evaluated the therapeutic potential of Drp1 deficiency in rats puncture-induced IVDD model (Fig. 3A). X-ray imaging showed significant collapse of disc height following puncture operation in the IVDD group, whereas treatment with si-Drp1 or Mdivi-1 resulted in a marked reduction of disc height collapse (Fig. 3B). The MRI examination revealed a decrease in the T2-weighted signal of the nucleus pulposus in punctured discs compared to those treated with si-Drp1 or Mdivi-1 (Fig. 3C). Gross examination of the discs suggested that the changes in disc height aligned with the X-ray findings, with more pronounced degenerative changes observed in discs with higher degeneration (Fig. 3D). Additionally, we observed significant infiltration of fibrous tissues into atrophic NP tissues and a distinct demarcation between NP and AF tissues in the IVDD group. However, treatment with si-Drp1 or Mdivi-1 partially reversed these histological alterations. The changes in degenerative pathology were consistent with the histological scoring, showing that the administration of si-Drp1 or Mdivi-1 significantly brought down the histological score compared to that of the IVDD group (Fig. 3E). These data suggested that Drp1 deficiency can effectively alleviate the progression of IVDD in rats puncture-induced IVDD model.

4.4. Drp1 deficiency alleviates oxidative stress-induced mitochondrial fission and mitochondria-dependent apoptosis in NPCs

Previous studies have suggested that mitochondrial homeostasis played an important role in regulating apoptosis. Drp1-mediated mitochondrial fission disrupts the balance of mitochondrial homeostasis, leading to excessive production of ROS [22,23]. We further investigated whether oxidative stress-induced Drp1-related mitochondrial fission was responsible for the increase of mitochondrial oxidative stress and mitochondria-dependent apoptosis. The NPCs were incubated with TBHP (40 μM, 24 h) to elevate the ROS level, while Mdivi-1 (10 μM, 24 h) was utilized to inhibit the activity of Drp1 [24].

The MitoTracker Red staining revealed an increased presence of tubular mitochondria following the knockdown or inhibition of Drp1, in

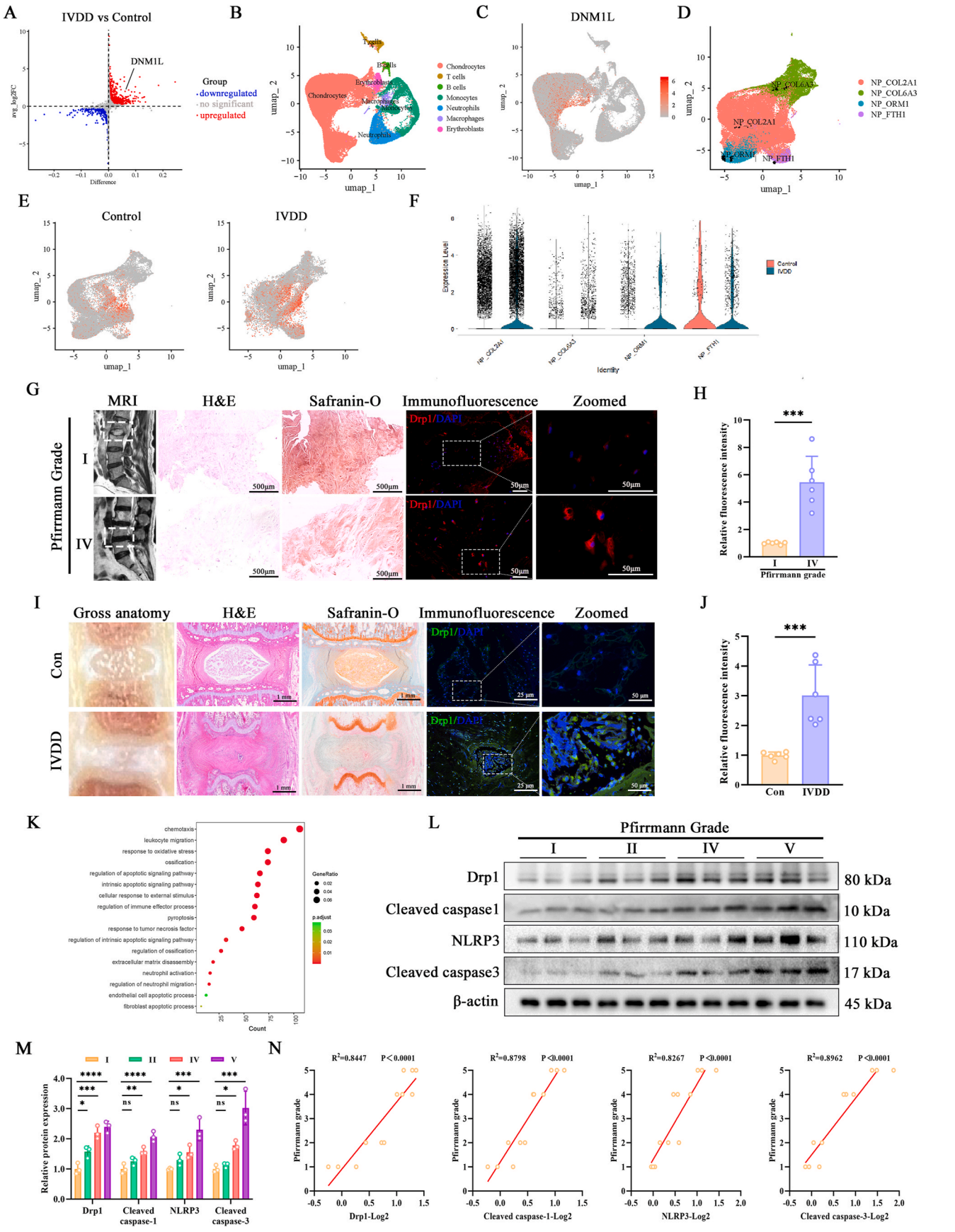

(caption on next page)

Fig. 1. Increased Drp1 expression, pyroptosis and apoptosis are involved in IVDD. (A) Volcano plot showing significantly up-regulated genes (red) and down-regulated genes (blue) in degenerative human nucleus pulposus (HNP) tissues compared with control. Differentially expressed genes (DEGs) were filtered by adjusted $p < 0.05$. (B) UMAP plot showing 7 clusters of cells in the human nucleus pulposus tissues, each plot represents one cell. (C) UMAP clustering showing the DNM1L (Drp1) distribution in the 7 different clusters. (D) UMAP visualizing 4 different clusters of human NPCs after clustering. (E, F) Gene expression of DNM1L in the 4 different clusters as shown by UMAP plot and scatter plot. (G) Representative MRI images, H&E staining, Safranin-O staining and immunofluorescence staining (Drp1) of Pfirrmann MRI degree I and IV HNP tissues. (H) Quantification of Drp1 fluorescence intensity in HNP tissue sections, n = 6. (I) Representative gross anatomy, H&E staining, Safranin-O staining and immunofluorescence staining (Drp1) of rats puncture-IVDD model. (J) Quantification of Drp1 fluorescence intensity in IVDD model, n = 6. (K) GO enrichment analysis of DEGs in different degenerative HNP tissues. (L, M) Western blot assay and quantification of Drp1, cleaved caspase-1, NLRP3 and cleaved caspase-3 in the different degrees HNP tissues according to the Pfirrmann grading system, n = 3. (N) Linear regression analysis between Drp1, cleaved caspase-1, NLRP3 or cleaved caspase-3 protein levels and Pfirrmann MRI grades. Data are shown as the mean ± SD. ns: no significance, *P < 0.05, **P < 0.01, ***P < 0.001, ****P < 0.0001.

contrast to the punctate structures observed in the TBHP group (Fig. 4A). Furthermore, the fluorescence intensity of MitoSOX increased markedly under TBHP treatment, but was attenuated following si-Drp1 or Mdivi-1 administration (Fig. 4B). Additionally, we examined the role of Drp1 in mitochondria-dependent apoptosis using western blot analysis and flow cytometry analysis of Annexin V/PI. Cleaved caspase-3, as the activated form of caspase-3, serves as a pivotal mediator of programmed cell death or apoptosis. Upon release from mitochondria under stress-induced damage, cytochrome c (cyt c) activates caspase-9, an upstream regulator of caspase-3. The western blot analysis indicated that both knockdown and inhibition of Drp1 significantly suppressed the translocation of cyt c from mitochondria to cytoplasm, leading to a decrease in cleaved caspase-3 expression (Fig. 4C and D). The flow cytometry revealed a marked reduction in the percentage of apoptotic NPCs following si-Drp1 or Mdivi-1 treatment (Fig. 4E and F). *In vivo*, TUNEL staining showed an increase in TUNEL positive cells in the rats puncture-induced IVDD model, which was then reversed by Drp1 deficiency (Fig. 4G and H). Similar trends were observed in immunohistochemical analysis of cleaved caspase-3 in these groups (Fig. 4I and J). These findings suggested that the increase of Drp1 expression was responsible for mitochondrial fission and mitochondria-dependent apoptosis in NPCs.

4.5. Drp1 deficiency inhibits pyroptosis in NPCs following TBHP treatment and in rats puncture-induced IVDD model

The effect of Drp1 deficiency on pyroptosis in NPCs was assessed following TBHP treatment and establishment of puncture-induced IVDD model. The western blot analysis indicated an up-regulation in the expression of pyroptosis markers (NLRP3, ASC, NT-GSDMD and cleaved caspase-1) upon TBHP treatment. However, this up-regulation was dramatically attenuated by the knockdown or pharmacological inhibition of Drp1 (Fig. 5A). IHC staining *in vitro* further supported the role of Drp1 deficiency in NLRP3 expression (Fig. 5B and C). Additionally, flow cytometry analysis was carried out for 7-AAD/caspase-1, revealing a reduction in the percentage of 7-AAD^{+}/caspase-1^{+} NPCs and indicating a mitigation of pyroptosis (Fig. 5D and E). Previous studies have suggested that oxidative stress induced mPTP opening and cytosolic mtDNA accumulation, leading to cGAS-Sting-NLRP3 pathway-dependent pyroptosis in NPCs [9,11]. In order to investigate whether oxidative stress induced mPTP opening via Drp1, we performed JC-1 staining to evaluate MMP, which was decreased by mPTP opening. We noted a significant reduction in JC-1 polymers and an increase in monomers upon Drp1 inhibition or knockdown (Fig. 5F and G). As the MMP decreased and mPTP increased, there was a concomitant rise in the release of cytosolic mtDNA from mitochondria. To verify the release of mtDNA, we carried out immunofluorescence staining using MitoTracker Red/dsDNA, which revealed a reduction in extra-mitochondrial mtDNA due to Drp1 deficiency (Fig. 5H and I). Finally, the therapeutic effect of si-Drp1 or Mdivi-1 on IVDD *in vitro* was identified by immunofluoresence staining which revealed reduced fluorescence intensity of NLRP3 with si-Drp1 or Mdivi-1 intervention (Fig. 5J and K). These findings collectively suggested that Drp1 deficiency inhibited pyroptosis in NPCs following TBHP treatment and in rats puncture-induced IVDD model.

4.6. Activation of ERK1/2 promotes Drp1 phosphorylation and mitochondrial translocation

The activation of Drp1 is regulated by a variety of post-translational modifications, including phosphorylation, SUMOylatiocd palmitoylation, etc. [25]. Among these modifications, phosphorylation stands out as one of the most crucial mechanisms [26]. Several phosphorylation sites on Drp1 have been identified, with the phosphorylation of Ser-616 playing a key role in the mitochondria translocation of Drp1 and subsequent mitochondrial fission [25]. In this study, immunofluorescence staining was performed to evaluate the phosphorylation status of Drp1 in HNP tissues. Our findings revealed a significant increase in the level of Drp1$^{Ser-616}$ phosphorylation in severely degenerated HNP tissues (Fig. 6A).

Previous studies have documented several upstream regulators of Drp1$^{Ser-616}$ phosphorylation, such as RIP1, ROCK, CaMKII, CDK1/cyclin B, and ERK1/2 [27,28]. Our prior studies also reported that ERK1/2 phosphorylation was activated in IL-1β-induced NPCs [29]. Additionally, through immunofluorescence staining of low and high degenerative HNP tissues, we confirmed that the levels of p-ERK1/2 increased in degenerative HNP tissues (Fig. 6B). In order to investigate whether Drp1$^{Ser-592}$ (the human equivalent of Drp1^{Ser616}) phosphorylation was regulated by p-ERK1/2 under oxidative stress, we cultured and treated the rat NPCs with TBHP (40 μM, 24 h). The ERK1/2 inhibitor PD98059 (2.5 μM) was utilized to inhibit ERK1/2 phosphorylation. The western blot analysis revealed that TBHP treatment up-regulated the expressions of p-ERK1/2 and p-Drp1$^{Ser-592}$, while the administration of PD98059 suppressed Drp1^{ser592} phosphorylation (Fig. 6C). To address the role of ERK1/2 in the translocation of Drp1 to the mitochondria, we performed immunofluorescence analysis on the co-localization of MitoTracker Red and Drp1. According to the images, a majority of Drp1 was located outside of the mitochondria in the negative group, while TBHP treatment induced a marked translocation of Drp1 from the cytoplasm to the mitochondria, a process that was suppressed by PD98059 (Fig. 6F). Additionally, the western blot analysis suggested that the inhibition of ERK1/2 with PD98059 attenuated TBHP-induced apoptosis and pyroptosis (Fig. 6D and E). These findings suggested that ERK1/2 activation triggered Drp1 phosphorylation and mitochondrial translocation, which mediated mitochondria-dependent apoptosis and pyroptosis.

5. Discussion

Drp1, as a multifunctional protein, plays a critical role in regulating various pathophysiological processes, including mitochondrial fission, metabolic reprogramming, apoptosis, pyroptosis, and autophagy [30,31]. Recent studies have reported elevated Drp1 expression in several degenerative diseases, such as Parkinson's disease, Alzheimer's disease and cardiovascular diseases [32,33]. While a large number of studies have reported that Drp1 activation contributes to NPC dysfunction, the role of Drp1 in IVDD remains poorly understood [15,34,35]. For this reason, it is essential to clarify whether Drp1 plays a key role in NPCs degeneration as well as IVDD for the purpose of further treatment.

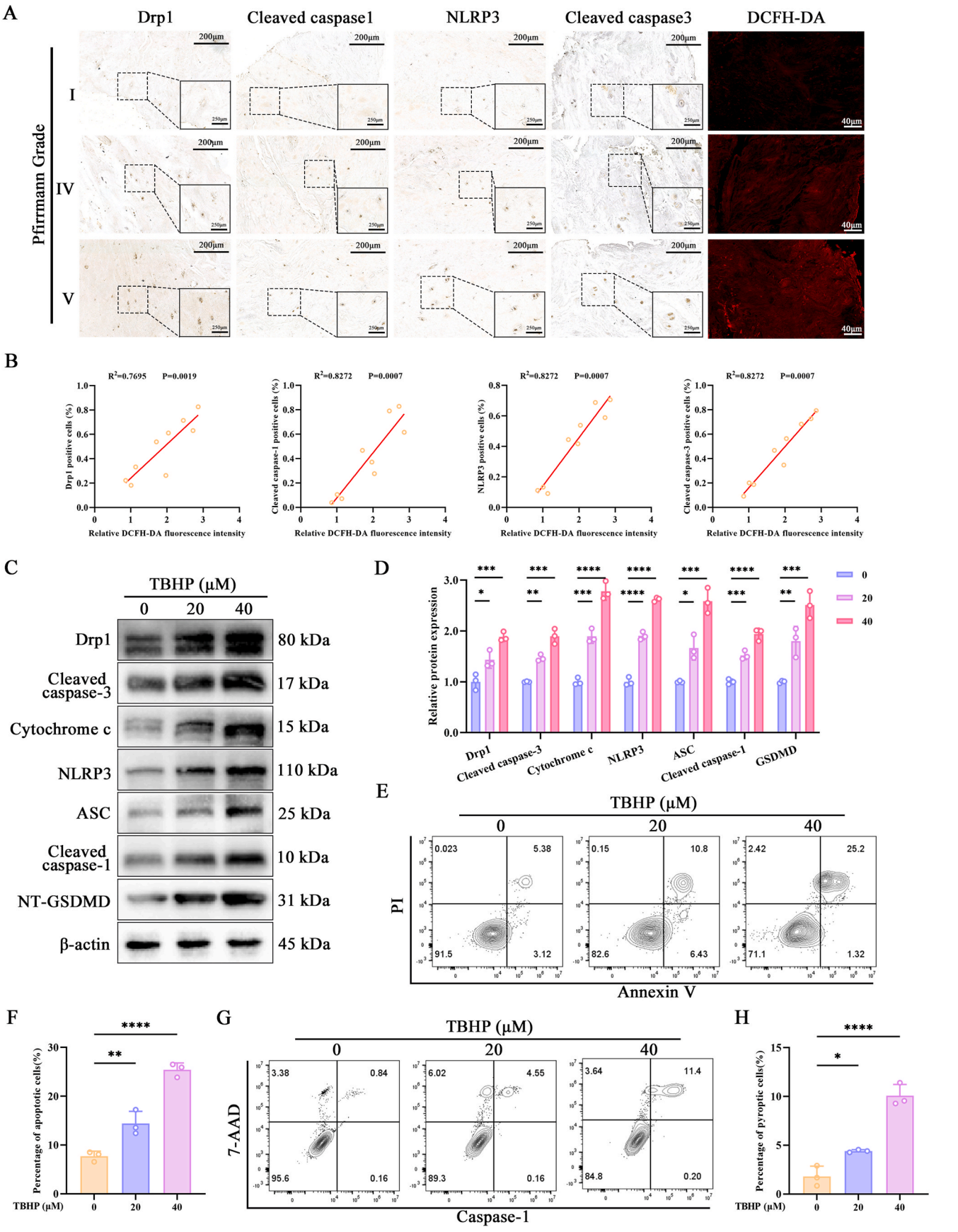

(caption on next page)

Fig. 2. Accumulated oxidative stress increases Drp1 expression and triggers pyroptosis and apoptosis in NPCs. NPCs were cultured and treated with 0, 20 and 40 μM TBHP for 24 h. (A) Immunohistochemistry (Drp1, cleaved caspase-1, NLRP3 and cleaved caspase-3) and DCFH-DA staining of human nucleus pulposus tissues with different degrees of degeneration, n = 3. (B) Linear regression analysis between protein levels of Drp1, cleaved caspase-1, NLRP3 or cleaved caspase-3 and ROS level of human nucleus pulposus tissues with different degrees of degeneration. (C, D) Western blot assay and quantification of Drp1, cleaved caspase-3, cttochrome c, NLRP3, ASC, cleaved caspase-1 and NT-GSDMD in NPCs treated with different concentrations of TBHP. (E) Annexin V/PI staining of NPCs treated with different concentrations of TBHP measured by flow cytometry. (F) The percentage of apoptotic cells measured by flow cytometry, n = 3. (G) Flow cytometry assay of caspase-1/7-AAD in NPCs treated with different concentrations of TBHP. (H) The percentage of pyroptotic cells measured by flow cytometry, n = 3. Data are shown as the mean ± SD. *P < 0.05, **P < 0.01, ***P < 0.001, ****P < 0.0001.

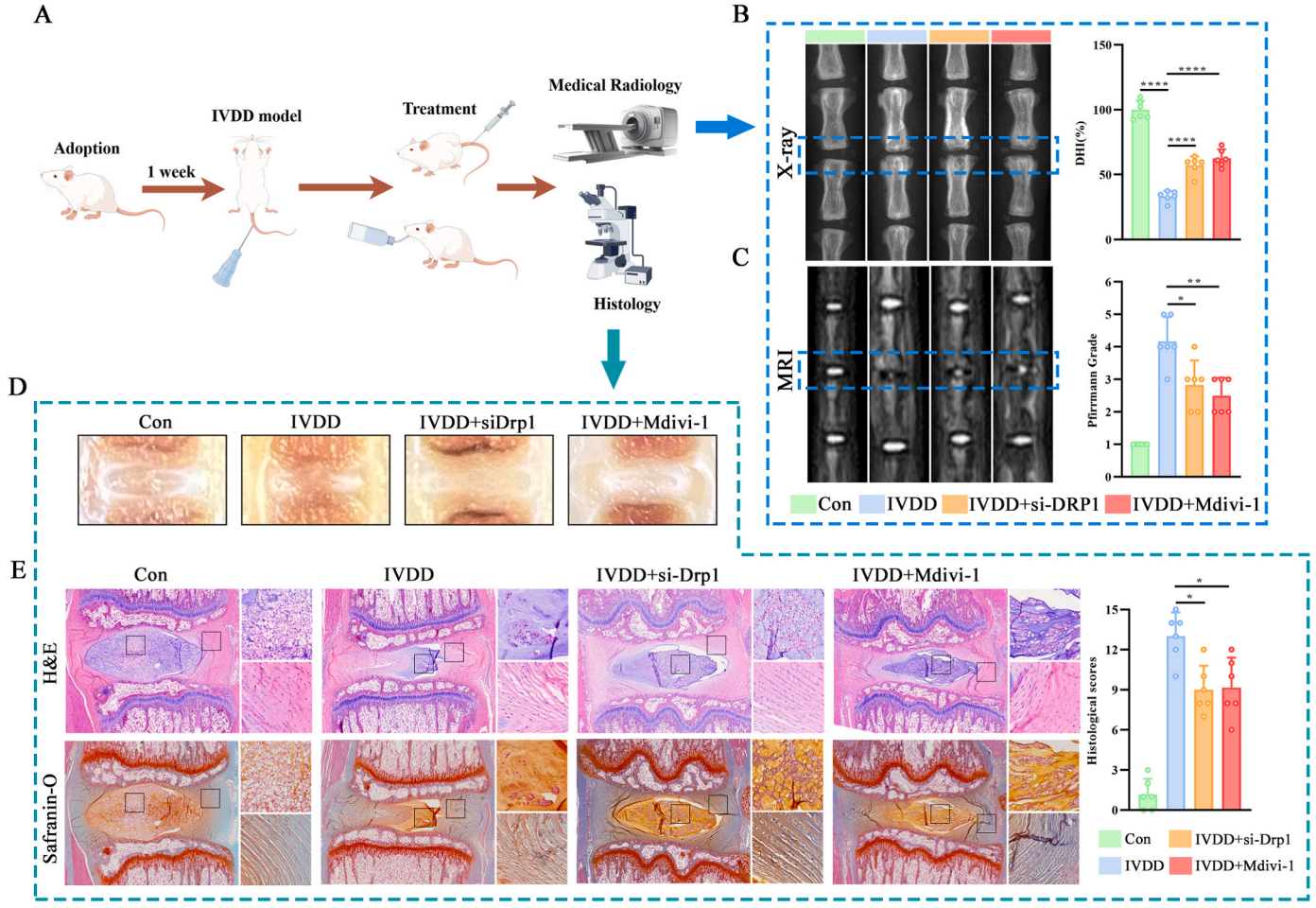

Fig. 3. Drp1 deficiency ameliorates rats puncture-IVDD progression. Rats puncture-IVDD model on Co7/8 was established, si-Drp1 intradiscally injection or Mdivi-1 intraperitoneally injection were conducted every week for 8 weeks. (A) The overview of the establishment and treatment of IVDD in rats model experiments. (B) The representative X-ray images and disc height index (DHI) analysis of the rat-tail discs at 8 weeks after surgery, n = 6. (C) The representative T2 weighted MRI images and Pfirrmann grade scores analysis of the rat-tail discs at 8 weeks after surgery, n = 6. (D) Representative gross anatomy images of disc samples from each group at 8 weeks after surgery. (E) Representative H&E and Safranin-O staining and histological score analysis of disc samples from each group at 8 weeks after surgery, n = 6. Data are shown as the mean ± SD. *P < 0.05, **P < 0.01, ****P < 0.0001.

The expression of Drp1 in NPCs has been a subject of debate in prior reports. Our previous study also showed that Drp1 expression was up-regulated in NPCs treated with IL-1β and TBHP [29]. Consistent with the findings reported by Peng et al., the expression of Drp1 in NPCs was markedly up-regulated by LPS intervention [36]. However, a more recent study found no significant difference in the levels of Drp1 protein between low degenerative (Pfirrmann Grade I and II) and high degenerative NP tissues (Pfirrmann Grade III and IV) NP tissues [34]. In the present study, we observed an up-regulation of Drp1 expression in degenerative NP tissues at both the mRNA and protein levels, which aligned with the findings from cellular experiments on NPCs exposed to oxidative stress. At the same time, a positive correlation was observed between the expression of Drp1 and the Pfirrmann MRI grade. These divergent results may be attributed to variations in sample sources, classification methods, and statistical methods.

Oxidative stress is a crucial pathological factor in IVDD [37]. The accumulation of ROS deteriorated mitochondrial dysfunction and apoptosis, accompanied by increased Drp1 expression. Nevertheless, the role of Drp1 in oxidative stress-induced apoptosis remains unclear. It has been reported that Drp1-mediated mitochondrial fission triggered mitochondrial dysfunction, characterized by increased mitochondrial ROS level [14,26]. Our study demonstrated that external oxidative stress can disrupt the anti-oxidative system, leading to an increase in mitochondrial ROS, as evidenced by mPTP opening and decreased MMP. These negative effect were alleviated by Drp1 deficiency with mild mitochondrial fragmentation. In chondrocytes, the pharmacological inhibition of Drp1 with Mdivi-1 suppressed IL-1β-induced mitochondrial fission and apoptosis [24]. Similarly, our study suggested that oxidative

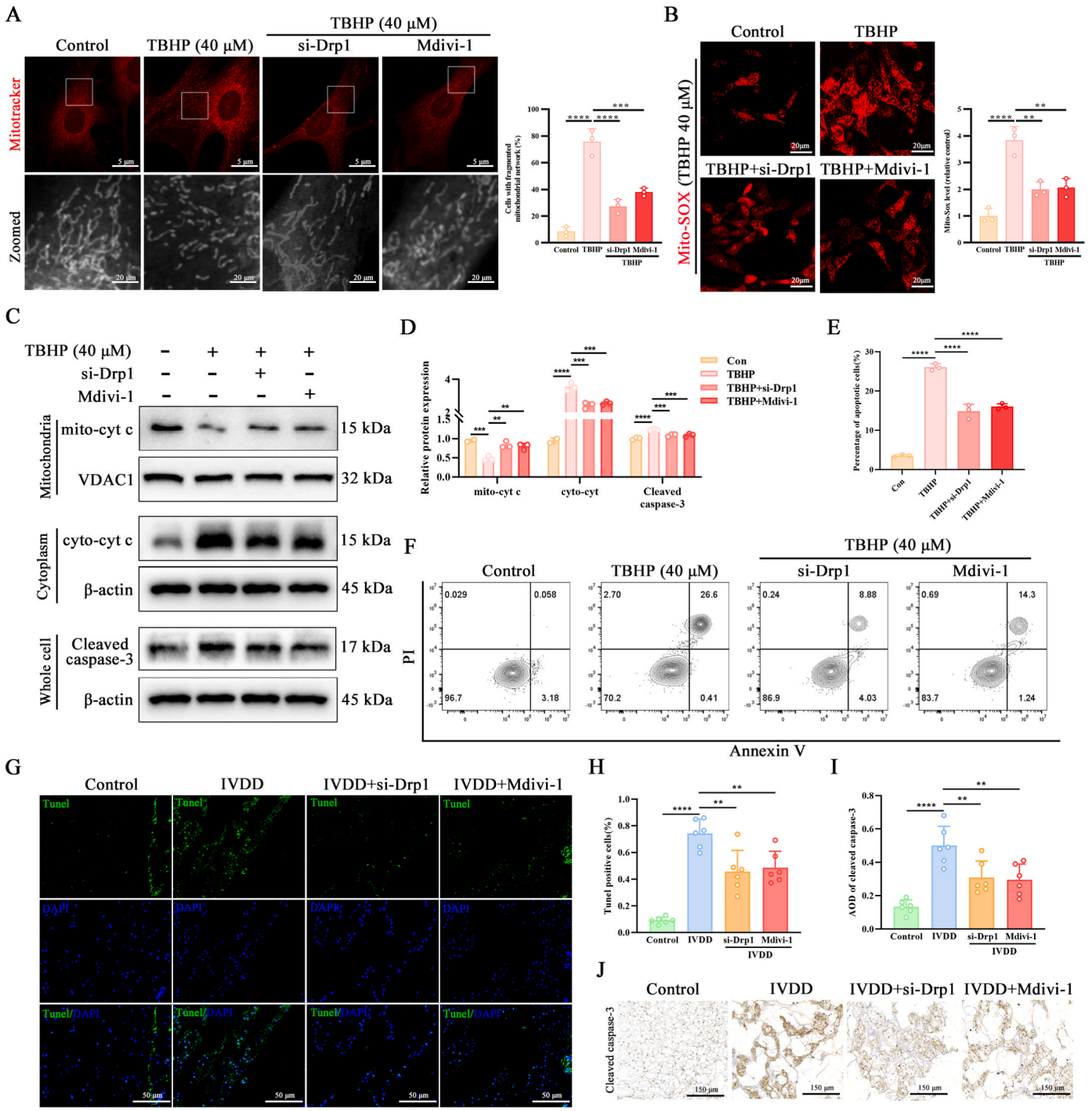

Fig. 4. Drp1 deficiency alleviates oxidative stress induced mitochondrial fission and mitochondria-dependent apoptosis in NPCs. NPCs were cultured and treated with si-Drp1 or Mdivi-1 in combination with 40 μM TBHP for 24 h. (A) Representative fluorescence images of mitochondria and analysis of fragmented mitochondrial network in NPCs, n = 3. (B) Representative fluorescence images and quantification of Mito-SOX in NPCs, n = 3. (C, D) Western blot analysis of the release of cytochrome c (cyt c) from mitochondria and protein level of cleaved caspase-3 in NPCs, n = 3. (E) Annexin V/PI staining of NPCs in the groups measured by flow cytometry. (F) The percentage of apoptotic cells measured by flow cytometry, n = 3. (G, H) Representative fluorescence images of Tunel staining of nucleus pulposus tissues and quantification of Tunel positive cells *in vivo*, n = 6. (I, J) Immunohistochemical staining and quantification of cleaved caspas-3 in nucleus pulposus tissues *in vivo*, n = 6. Data are shown as the mean ± SD. **P < 0.01, ***P < 0.001, ****P < 0.0001.

stress can accelerate Drp1-dependent intrinsic apoptosis. This was probably attributed to previous reports that revealed that Drp1 activated Bax oligomerization, interacted with the Bax/Bak complex to form mitochondrial pores, a crucial step in cytochrome c release into the cytoplasm activating the apoptosis process [38,39].

Oxidative stress not only disrupts the microenvironment of NPCs, but also triggers pyroptosis in NPCs [40]. NPCs pyroptosis promotes inflammatory response, expediting extracellular matrix degradation, further impairing the physiological functions of NPCs. The NLRP3 inflammasome, consisting of NLRP3, ASC, and caspase-1, activates GSDMD-mediated pyroptosis via activated caspase-1. Previous studies have reported that NLRP3-mediated pyroptosis was involved in the pathogenesis of IVDD [21]. Under oxidative stress, MMP decreased, leading to mPTP opening and release of damaged dsDNA from the

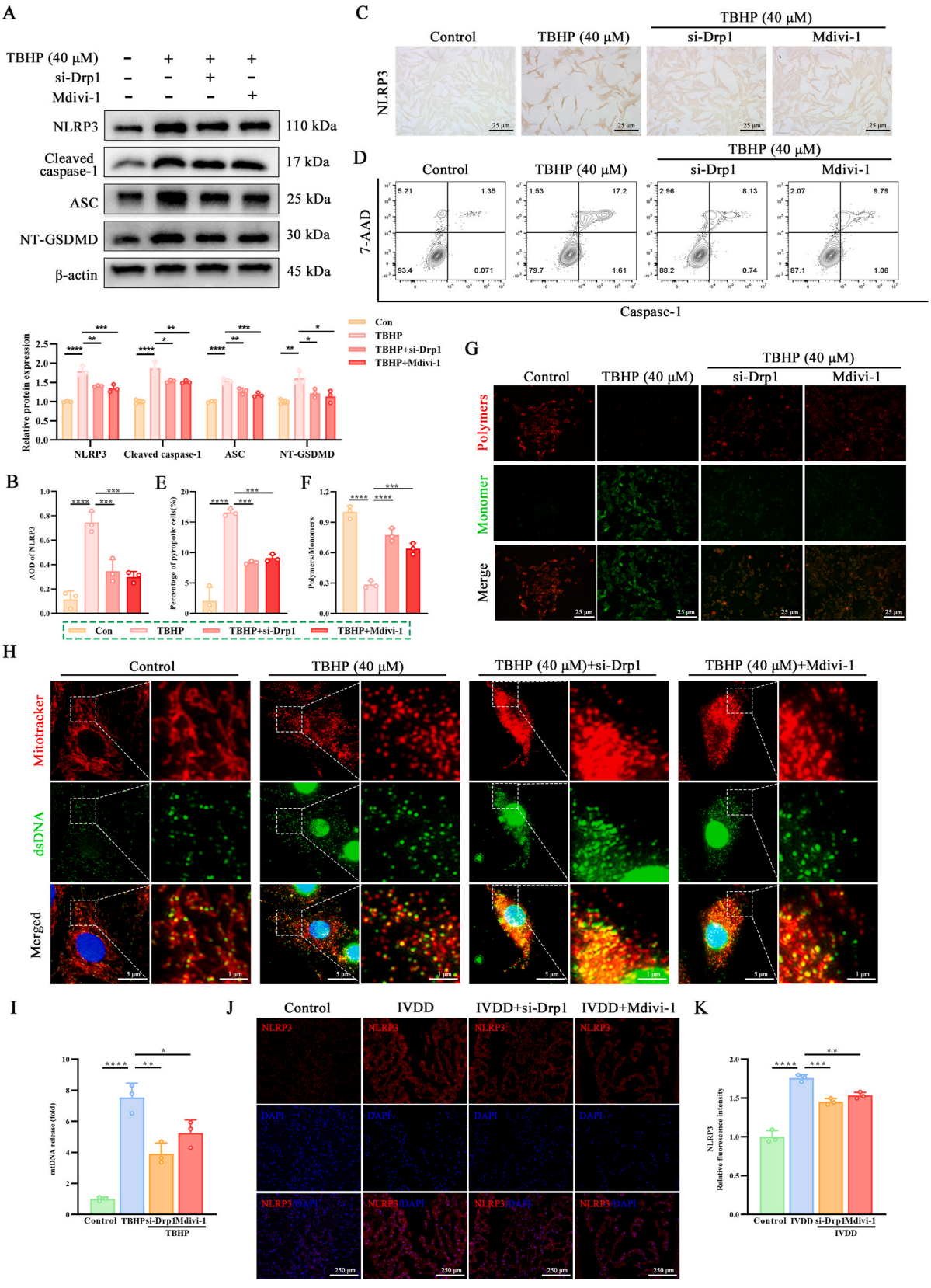

Fig. 5. Drp1 deficiency suppresses pyroptosis in TBHP treated NPCs and IVDD model. NPCs were cultured and treated with si-Drp1 or Mdivi-1 in combination with 40 μM TBHP for 24 h. (A) Western blot analysis of protein levels of NLRP3, cleaved caspase-1, ASC and NT-GSDMD in NPCs, n = 3. (B, C) Immunohistochemical images and quantification of NLRP3 intensity in NPCs, n = 3. (D, E) Caspase-1/7-AAD staining and the percentage of pyroptotic cells measured by flow cytometry, n = 3. (F, G) JC-1 staining assay and quantification of NPCs in each group. (H, I) Representative fluorescence images of mitochondria (red), dsDNA (green) and nucleus (blue) and quantification of mtDNA release in the pre-treated NPCs. (J, K) Immunofluorescence assay and analysis of NLRP3 in nucleus pulposus tissues in IVDD model, n = 6. Data are shown as the mean ± SD. *P < 0.05, **P < 0.01, ***P < 0.001, ****P < 0.0001.

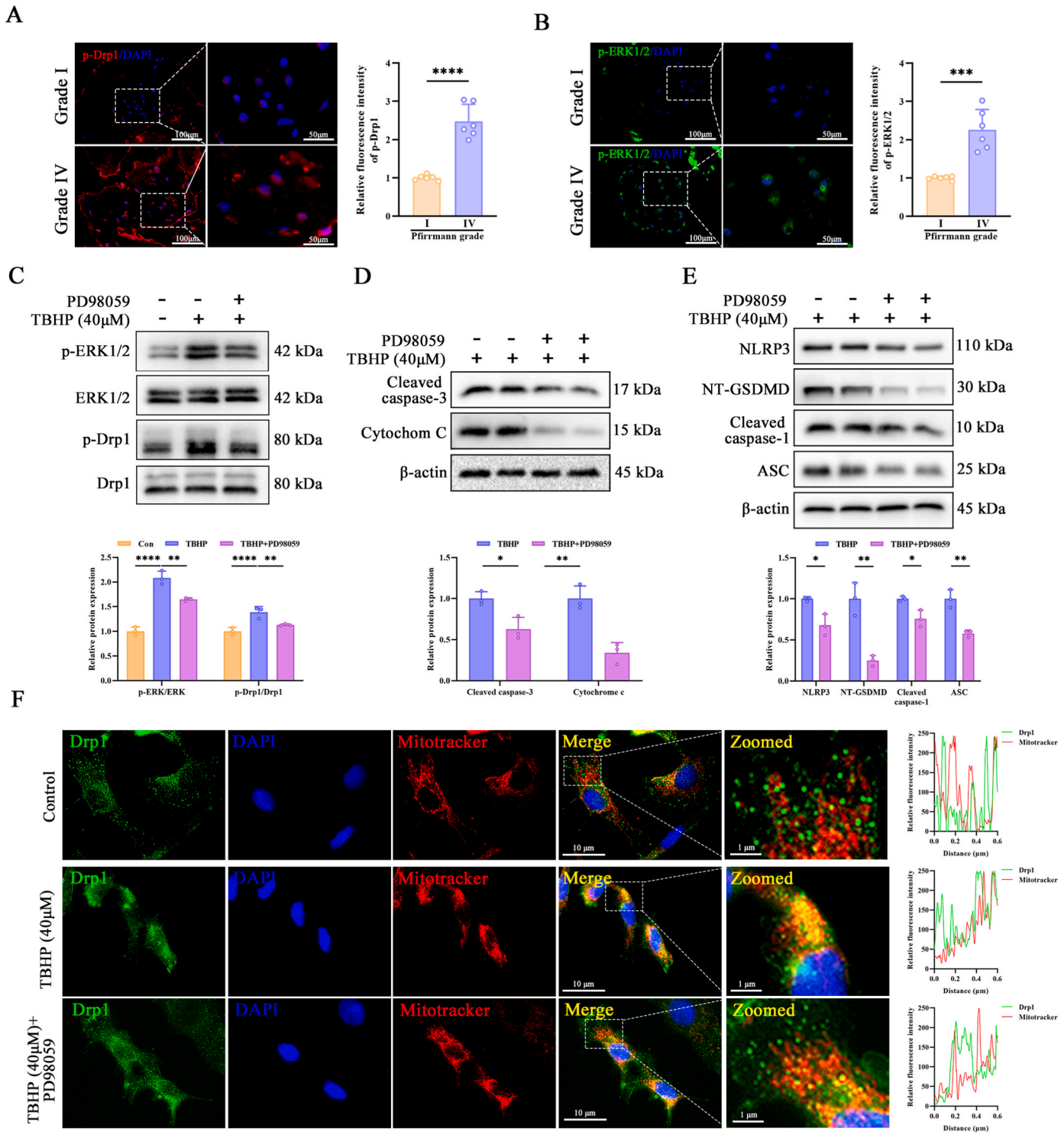

Fig. 6. Activation of ERK1/2 promotes Drp1 phosphorylation and mitochondrial translocation. In cellular experiments, ERK1/2 inhibitor PD98059 was used to suppress ERK1/2 phosphorylation in NPCs treated with TBHP (40 μM) in 24 h. (A) Immunofluorescence staining and analysis of p-Drp1 fluorescence intensity in human nucleus pulposus tissues with Pfirrmann MRI grade I and IV, n = 6. (B) Immunofluorescence staining and analysis of p-ERK1/2 fluorescence intensity in human nucleus pulposus tissues with Pfirrmann MRI grade I and IV, n = 6. (C) Western blot assay and quantification of the protein levels of p-ERK1/2 and p-Drp1 in NPCs, n = 3. (D) Western blot assay and quantification of the protein levels of cleaved caspase-3 and cytochrome c in NPCs, n = 3. (E) Western blot assay and quantification of the protein levels of NLRP3, NT-GSDMD, cleaved caspase-1 and ASC in NPCs, n = 3. (F) Representative fluorescence images of Drp1 (green), mitochondria (red) and nucleus (blue) in NPCs. Data are shown as the mean ± SD. *P < 0.05, **P < 0.01, ***P < 0.001, ****P < 0.0001.

mitochondria into the cytoplasm [41,42] Although AIM2 is a sensor of dsDNA in the cytoplasm, cytoplasmic dsDNA in NPCs is predominantly recognized by the DNA receptor cGAS [10,43]. The activation of cGAS-Sting-NLRP3 axis subsequently triggers pyroptosis in NPCs, while the pharmacological inhibition of mPTP diminishes the release of mtDNA into the cytoplasm and suppresses the mtDNA-cGAS-Sting-NLRP3 axis-mediated pyroptotic response [11]. In this study, we found that knockdown and inhibition of Drp1 improved

abnormal mitochondrial fission, attenuated MMP decrease, reduced mtDNA release from mitochondria into cytoplasm, and alleviated oxidative stress-induced pyroptosis in NPCs.

The activity of Drp1 is regulated by a variety of post-translational modifications, which plays a crucial role in the modulation of Drp1 activity, protein stability, GTPase activity, and translocation between the mitochondria and cytoplasm [44]. Among these post-translational modifications, phosphorylation has garnered significant attention because of its functional implications. The protein Drp1 possesses multiple phosphorylation sites, with two primary sites, Ser-616 and Ser-637, being extensively studied for their distinct functions [14,26,45]. Especially the phosphorylation of Ser-616 facilitates mitochondrial fission, which is regulated by upstream phosphokinases, including CDK1, CaMKII and ERK1/2 [27,28,46]. Our previous study revealed an up-regulation of ERK1/2 phosphorylation in IL-1β-treated NPCs [29]. A recent study also reported that Piezol1 facilitates $Drp1^{ser-616}$ phosphorylation by activating ERK1/2 in response to matrix stiffness, thereby promoting the translocation of Drp1 to mitochondria and subsequent NPCs apoptosis [34]. In the present study, we observed a marked increase of the phosphorylation level of ERK1/2 in severely degenerative HNP tissues. In addition, our *in vitro* experiments confirmed that p-ERK1/2 was significantly up-regulated in NPCs under oxidative stress. Treatment with the ERK inhibitor PD98059 effectively mitigated oxidative stress-induced Drp1 phosphorylation, inhibited Drp1 translocation to the mitochondria, and suppressed both apoptosis and pyroptosis in NPCs.

Several limitations are evident in this study. First of all, the exact mechanism through which Drp1 facilitates mPTP opening remains incompletely elucidated in this study. Secondly, although previous studies have highlighted a potential correlation between mitophagy and mitochondrial fission, our study does not delve into the connection between Drp1 and mitophagy. Furthermore, the role of other phosphokinases than ERK1/2 in the regulation of Drp1 activity also warrants further investigation.

In conclusion, our study demonstrates that the up-regulation of Drp1 in NPCs is correlated with the severity of IVDD. Specifically, increased phosphorylation of Drp1 can contribute to apoptosis and pyroptosis in NPCs. In addition, treatment with the Drp1 inhibitor Mdivi-1 shows potential in alleviating IVDD both *in vitro* and *in vivo*. These findings offer deeper insights into the molecular mechanisms underlying IVDD, suggesting that Drp1 may serve a potential therapeutic target in IVDD, and Mdivi-1 holds promise as a potential candidate for IVDD treatment.

Data availability

The data that support the findings of this study are available from the corresponding author upon reasonable request.

Declaration of competing interest

The authors declare no conflict of interest in the study.

Acknowledgments

This work is supported by grants from Science and Technology Plan Project of Wenzhou Municipality, China (Y2020051), Zhejiang Provincial Project for Medical and Health Science and Technology, China (2021KY796), Basic Scientific Research Business of Wenzhou Medical University, China (KYYW202232).

Appendix A. Supplementary data

Supplementary data to this article can be found online at https://doi.org/10.1016/j.jot.2025.01.013.

References

[1] Hartvigsen J, Hancock M, Kongsted A, Louw Q, Ferreira M, Genevay S, et al. What low back pain is and why we need to pay attention. Lancet (London, England) 2018;391(10137):2356–67.
[2] Gbdlbp Collaborators. Global, regional, and national burden of low back pain, 1990-2020, its attributable risk factors, and projections to 2050: a systematic analysis of the Global Burden of Disease Study 2021. Lancet Rheumatol 2023;5(6):e316–29.
[3] Kang L, Zhang H, Jia C, Zhang R, Shen C. Epigenetic modifications of inflammation in intervertebral disc degeneration. Ageing Res Rev 2023;87:101902.
[4] Kummer E, Ban N. Mechanisms and regulation of protein synthesis in mitochondria. Nat Rev Mol Cell Biol 2021;22(5):307–25.
[5] Fromenty B, Roden M. Mitochondrial alterations in fatty liver diseases. J Hepatol 2023;78(2):415–29.
[6] Wang J, Zhang J, Yu ZL, Chung SK, Xu B. The roles of dietary polyphenols at crosstalk between type 2 diabetes and Alzheimer's disease in ameliorating oxidative stress and mitochondrial dysfunction via PI3K/Akt signaling pathways. Ageing Res Rev 2024;99:102416.
[7] Vringer E, Tait SWG. Mitochondria and cell death-associated inflammation. Cell Death Differ 2023;30(2):304–12.
[8] Motwani M, Pesiridis S, Fitzgerald KA. DNA sensing by the cGAS-STING pathway in health and disease. Nat Rev Genet 2019;20(11):657–74.
[9] Zhang W, Li G, Zhou X, Liang H, Tong B, Wu D, et al. Disassembly of the TRIM56-ATR complex promotes cytoDNA/cGAS/STING axis-dependent intervertebral disc inflammatory degeneration. J Clin Invest 2024;134(6).
[10] Guo Q, Zhu D, Wang Y, Miao Z, Chen Z, Lin Z, et al. Targeting STING attenuates ROS induced intervertebral disc degeneration. Osteoarthritis Cartilage 2021;29(8):1213–24.
[11] Zhang W, Li G, Luo R, Lei J, Song Y, Wang B, et al. Cytosolic escape of mitochondrial DNA triggers cGAS-STING-NLRP3 axis-dependent nucleus pulposus cell pyroptosis. Exp Mol Med 2022;54(2):129–42.
[12] Fu W, Liu Y, Yin H. Mitochondrial dynamics: biogenesis, fission, fusion, and mitophagy in the regulation of stem cell behaviors. Stem Cells Int 2019;2019:9757201.
[13] Kraus F, Roy K, Pucadyil TJ, Ryan MT. Function and regulation of the divisome for mitochondrial fission. Nature 2021;590(7844):57–66.
[14] Rosdah AA, Smiles WJ, Oakhill JS, Scott JW, Langendorf CG, Delbridge LMD, et al. New perspectives on the role of Drp1 isoforms in regulating mitochondrial pathophysiology. Pharmacol Ther 2020;213:107594.
[15] Lin Z, Wang H, Song J, Xu G, Lu F, Ma X, et al. The role of mitochondrial fission in intervertebral disc degeneration. Osteoarthritis Cartilage 2023;31(2):158–66.
[16] Sun K, Yan C, Dai X, Shi Y, Li F, Chen L, et al. Catalytic nanodots-driven pyroptosis suppression in nucleus pulposus for antioxidant intervention of intervertebral disc degeneration. Adv Mater 2024;36(19):e2313248.
[17] Chen Q, Qian Q, Xu H, Zhou H, Chen L, Shao N, et al. Mitochondrial-targeted metal-phenolic nanoparticles to attenuate intervertebral disc degeneration: alleviating oxidative stress and mitochondrial dysfunction. ACS Nano 2024;18(12):8885–905.
[18] Riley JS, Quarato G, Cloix C, Lopez J, O'Prey J, Pearson M, et al. Mitochondrial inner membrane permeabilisation enables mtDNA release during apoptosis. EMBO J 2018;37(17).
[19] Zeng Z, You M, Fan C, Rong R, Li H, Xia X. Pathologically high intraocular pressure induces mitochondrial dysfunction through Drp1 and leads to retinal ganglion cell PANoptosis in glaucoma. Redox Biol 2023;62:102687.
[20] Zheng G, Pan Z, Zhan Y, Tang Q, Zheng F, Zhou Y, et al. TFEB protects nucleus pulposus cells against apoptosis and senescence via restoring autophagic flux. Osteoarthritis Cartilage 2019;27(2):347–57.
[21] Zhou J, Qiu J, Song Y, Liang T, Liu S, Ren C, et al. Pyroptosis and degenerative diseases of the elderly. Cell Death Dis 2023;14(2):94.
[22] Li J, Chang X, Shang M, Niu S, Zhang W, Li Y, et al. The crosstalk between DRP1-dependent mitochondrial fission and oxidative stress triggers hepatocyte apoptosis induced by silver nanoparticles. Nanoscale 2021;13(28):12356–69.
[23] Romani P, Nirchio N, Arboit M, Barbieri V, Tosi A, Michielin F, et al. Mitochondrial fission links ECM mechanotransduction to metabolic redox homeostasis and metastatic chemotherapy resistance. Nat Cell Biol 2022;24(2):168–80.
[24] Ansari MY, Novak K, Haqqi TM. ERK1/2-mediated activation of DRP1 regulates mitochondrial dynamics and apoptosis in chondrocytes. Osteoarthritis Cartilage 2022;30(2):315–28.
[25] Jin JY, Wei XX, Zhi XL, Wang XH, Meng D. Drp1-dependent mitochondrial fission in cardiovascular disease. Acta Pharmacol Sin 2021;42(5):655–64.
[26] Rahmani S, Roohbakhsh A, Karimi G. Inhibition of Drp1-dependent mitochondrial fission by natural compounds as a therapeutic strategy for organ injuries. Pharmacol Res 2023;188:106672.
[27] Bo T, Yamamori T, Suzuki M, Sakai Y, Yamamoto K, Inanami O. Calmodulin-dependent protein kinase II (CaMKII) mediates radiation-induced mitochondrial fission by regulating the phosphorylation of dynamin-related protein 1 (Drp1) at serine 616. Biochem Biophys Res Commun 2018;495(2):1601–7.
[28] Adaniya SM, J OU, Cypress MW, Kusakari Y, Jhun BS. Posttranslational modifications of mitochondrial fission and fusion proteins in cardiac physiology and pathophysiology. Am J Physiol Cell Physiol 2019;316(5):C583–604.
[29] Xu D, Jin H, Wen J, Chen J, Chen D, Cai N, et al. Hydrogen sulfide protects against endoplasmic reticulum stress and mitochondrial injury in nucleus pulposus cells and ameliorates intervertebral disc degeneration. Pharmacol Res 2017;117:357–69.

[30] Rosdah A, Smiles W, Oakhill J, Scott J, Langendorf C, Delbridge L, et al. New perspectives on the role of Drp1 isoforms in regulating mitochondrial pathophysiology. Pharmacology & therapeutics 2020;213:107594.
[31] Casuso R, Huertas J. The emerging role of skeletal muscle mitochondrial dynamics in exercise and ageing. Ageing Res Rev 2020;58:101025.
[32] Rajendran K, Krishnan UM. Mechanistic insights and emerging therapeutic stratagems for Alzheimer's disease. Ageing Res Rev 2024;97:102309.
[33] Quiles JM, Gustafsson AB. The role of mitochondrial fission in cardiovascular health and disease. Nat Rev Cardiol 2022;19(11):723–36.
[34] Ke W, Wang B, Liao Z, Song Y, Li G, Ma L, et al. Matrix stiffness induces Drp1-mediated mitochondrial fission through Piezo1 mechanotransduction in human intervertebral disc degeneration. J Transl Med 2023;21(1):711.
[35] Wu W, Jing D, Huang X, Yang W, Shao Z. Drp1-mediated mitochondrial fission is involved in oxidized low-density lipoprotein-induced AF cella poptosis. J Orthop Res : official publication of the Orthopaedic Research Society 2021;39(7):1496–504.
[36] Peng X, Zhang C, Zhou ZM, Wang K, Gao JW, Qian ZY, et al. A20 attenuates pyroptosis and apoptosis in nucleus pulposus cells via promoting mitophagy and stabilizing mitochondrial dynamics. Inflamm Res 2022;71(5–6):695–710.
[37] Zhou H, Wu C, Jin Y, Wu O, Chen L, Guo Z, et al. Role of oxidative stress in mitochondrial dysfunction and their implications in intervertebral disc degeneration: mechanisms and therapeutic strategies. Journal of orthopaedic translation 2024;49:181–206.
[38] Jenner A, Pena-Blanco A, Salvador-Gallego R, Ugarte-Uribe B, Zollo C, Ganief T, et al. DRP1 interacts directly with BAX to induce its activation and apoptosis. EMBO J 2022;41(8):e108587.
[39] Grosse L, Wurm CA, Bruser C, Neumann D, Jans DC, Jakobs S. Bax assembles into large ring-like structures remodeling the mitochondrial outer membrane in apoptosis. EMBO J 2016;35(4):402–13.
[40] Xing H, Zhang Z, Mao Q, Wang C, Zhou Y, Zhou X, et al. Injectable exosome-functionalized extracellular matrix hydrogel for metabolism balance and pyroptosis regulation in intervertebral disc degeneration. J Nanobiotechnology 2021;19(1):264.
[41] Kim J, Gupta R, Blanco LP, Yang S, Shteinfer-Kuzmine A, Wang K, et al. VDAC oligomers form mitochondrial pores to release mtDNA fragments and promote lupus-like disease. Science 2019;366(6472):1531–6.
[42] Matsui H, Ito J, Matsui N, Uechi T, Onodera O, Kakita A. Cytosolic dsDNA of mitochondrial origin induces cytotoxicity and neurodegeneration in cellular and zebrafish models of Parkinson's disease. Nat Commun 2021;12(1):3101.
[43] Gu F, Wang Z, Ding H, Tao X, Zhang J, Dai K, et al. Microglial mitochondrial DNA release contributes to neuroinflammation after intracerebral hemorrhage through activating AIM2 inflammasome. Exp Neurol 2024:114950.
[44] Simula L, Campanella M, Campello S. Targeting Drp1 and mitochondrial fission for therapeutic immune modulation. Pharmacol Res 2019;146:104317.
[45] Miotto PM, Dao GM, Brunetta HS. Fission accomplished: uncovering the role of Drp1 in regulating mitochondrial dysfunction and age-related muscle atrophy. J Physiol 2021;599(21):4745–7.
[46] Cho B, Choi SY, Cho HM, Kim HJ, Sun W. Physiological and pathological significance of dynamin-related protein 1 (drp1)-dependent mitochondrial fission in the nervous system. Exp Neurobiol 2013;22(3):149–57.